

# Analysis of Neuroretinal Rim by Age, Race, and Sex Using High-Density 3-Dimensional Spectral-Domain Optical Coherence Tomography

Hussein Antar, BS,\*† Edem Tsikata, PhD,†‡  
 Kitiya Ratanawongphaibul, MD,†‡§ Jing Zhang, MD,†|| Eric Shieh, MD,†¶  
 Ramon Lee, MD,†# Madeline Freeman, LCSW,†\*\*  
 Georgia Papadogeorgou, PhD,†† Huseyin Simavli, MD,†‡‡  
 Christian Que, MD,†§§ Alice C. Verticchio Vercellin, MD,†|||¶¶  
 Ziad Khoueir, MD,†‡##\*\*\* Johannes F. de Boer, PhD,†††‡‡‡  
 and Teresa C. Chen, MD†‡

**Précis:** Neuroretinal rim minimum distance band (MDB) thickness is significantly lower in older subjects and African Americans compared with whites. It is similar in both sexes.

**Purpose:** To evaluate the relationship between age, race, and sex with the neuroretinal rim using high-density spectral-domain optical coherence tomography optic nerve volume scans of normal eyes.

**Methods:** A total of 256 normal subjects underwent Spectralis spectral-domain optical coherence tomography optic nerve head volume

scans. One eye was randomly selected and analyzed for each subject. Using custom-designed software, the neuroretinal rim MDB thickness was calculated from volume scans, and global and quadrant neuroretinal rim thickness values were determined. The MDB is a 3-dimensional neuroretinal rim band comprised of the shortest distance between the internal limiting membrane and the termination of the retinal pigment epithelium/Bruch's membrane complex. Multiple linear regression analysis was performed to determine the associations of age, race, and sex with neuroretinal rim MDB measurements.

**Results:** The population was 57% female and 69% white with a mean age of  $58.4 \pm 15.3$  years. The mean MDB thickness in the normal population was  $278.4 \pm 47.5 \mu\text{m}$ . For this normal population, MDB thickness decreased by  $0.84 \mu\text{m}$  annually ( $P < 0.001$ ). African Americans had thinner MDBs compared with whites ( $P = 0.003$ ). Males and females had similar MDB thickness values ( $P = 0.349$ ).

**Conclusion:** Neuroretinal rim MDB thickness measurements decreased significantly with age. African Americans had thinner MDB neuroretinal rims than whites.

**Key Words:** optical coherence tomography, neuroretinal rim, optic nerve

(*J Glaucoma* 2019;28:979–988)

Received for publication December 29, 2018; accepted September 16, 2019.

From the \*University of Massachusetts Medical School, Worcester; †Department of Ophthalmology, Massachusetts Eye and Ear Infirmary; ‡Harvard Medical School, Boston; \*\*Smith College School for Social Work, Northampton, MA; §Department of Ophthalmology, King Chulalongkorn Memorial Hospital, Bangkok, Thailand; ||Department of Ophthalmology, Peking University First Hospital, Beijing, China; ¶Jules Stein Eye Institute, UCLA; #University of Southern California Roski Eye Institute, Los Angeles, CA; ††Department of Statistical Science, Duke University, Durham, NC; ‡‡Kudret Private Eye Hospital, Istanbul, Turkey; §§University of the East Ramon Magsaysay Memorial Medical Center, Manila, Philippines; |||Glaucoma Unit, Institute for Treatment and Research, G.B. Bietti Foundation; ¶¶University of Pavia, Pavia, Italy; ##Beirut Eye and ENT Specialist Hospital; \*\*\*Ophthalmology Department, Saint-Joseph University, Beirut, Lebanon; †††LaserLaB Amsterdam, Department of Physics and Astronomy, Vrije Universiteit; and ‡‡‡Department of Ophthalmology, VU Medical Center, Amsterdam, The Netherlands.

Disclosure: J.F.d.B. is the chair of the Scientific Advisory Board of the Center for Biomedical Optical Coherence Tomography Research and Translation (Harvard Medical School), and licenses to NIDEK Inc., Terumo Corporation, Ninepoint Medical, and Heidelberg Engineering, outside the submitted work. T.C.C. received funding from the following: American Glaucoma Society Mid-Career Award (San Francisco, CA), Massachusetts Lions Eye Research Fund, Fidelity Charitable Fund (Harvard University, Boston, MA), Harvard Catalyst Grant, National Institutes of Health UL RR025758 (Bethesda, MD), and Department of Defense Small Business Innovation Research DHP15-016. The remaining authors declare no conflict of interest.

Reprints: Teresa C. Chen, MD, Department of Ophthalmology, Harvard Medical School, Massachusetts Eye and Ear Infirmary, Glaucoma Service, 243 Charles Street, Boston, MA 02114 (e-mail: teresa\_chen@meei.harvard.edu).

Copyright © 2019 The Author(s). Published by Wolters Kluwer Health, Inc. This is an open-access article distributed under the terms of the Creative Commons Attribution-Non Commercial-No Derivatives License 4.0 (CCBY-NC-ND), where it is permissible to download and share the work provided it is properly cited. The work cannot be changed in any way or used commercially without permission from the journal.  
 DOI: 10.1097/IJG.0000000000001381

Spectral-domain optical coherence tomography (SD-OCT) has become an integral part of the clinical evaluation for glaucoma because it can objectively measure the neuroretinal rim, the ganglion cell region, and the retinal nerve fiber layer (RNFL), all of which are known to decrease with glaucoma.<sup>1–12</sup> As optical coherence tomography (OCT) imaging can show structural changes years before functional visual field (VF) loss, structural tests remain a cornerstone in the evaluation of glaucoma patients.<sup>13–16</sup> However, clinicians who use neuroretinal rim structural tests need to be aware of how much nerve tissue loss is expected for normal aging and how much racial variation exists in SD-OCT parameters to distinguish normal aging changes and racial variation from glaucomatous changes.

Most SD-OCT studies that look at the effect of age, race, and sex on structural parameters have focused on RNFL thickness.<sup>10–12,17–23</sup> These studies have found that increasing age is associated with RNFL thickness decreases between 0.18 and  $0.44 \mu\text{m}$  annually in normal adult patients.<sup>10–12,17–21</sup>

Multiple studies reported that sex is not significantly correlated with RNFL thickness,<sup>19,22,23</sup> whereas 1 reported that women had thicker RNFL than men.<sup>24</sup> Two studies reported that whites had thinner RNFL thickness measurements than other racial groups.<sup>18,19</sup> However, RNFL thickness measurements through SD-OCT have a high rate of imaging artifacts, and up to 46.3% of RNFL thickness scans have artifacts, which can be caused by decentration errors, posterior vitreous detachments, and epiretinal membranes.<sup>25,26</sup>

In contrast, SD-OCT studies which look at the effect of age, race, and sex on the neuroretinal rim are few and are limited to 2 studies which used a low-density scan protocol and evaluated the Bruch membrane opening minimum rim width (BMO-MRW) parameter, which has not been consistently shown to be diagnostically better than the RNFL thickness parameter.<sup>22,23,27</sup> To our knowledge, there are no SD-OCT studies which use a high-density scan protocol to evaluate the effects of age, race, and sex on the neuroretinal rim. Therefore, this current study utilizes the minimum distance band (MDB) neuroretinal parameter, which is derived from high-density optic nerve scans and which has been shown to be diagnostically better than RNFL thickness, especially in the nasal, temporal, and superonasal regions.<sup>28-30</sup> The reproducibility of MDB thickness is high, with an inter-test variability of 0.84%.<sup>28</sup> Like other 3-dimensional (3D) neuroretinal rim parameters, the MDB thickness uses SD-OCT imaging to determine the borders of the neuroretinal rim. These other 3D parameters include the minimum circumpapillary band, which defines the neuroretinal rim as the distance between the

internal limiting membrane (ILM) and the retinal pigment epithelium (RPE),<sup>31</sup> and the BMO-MRW, which defines the neuroretinal rim as the distance between the ILM and the BMO.<sup>22,23,27</sup> However, although Bruch membrane (BM) may be visible on SD-OCT, it is often indistinguishable from the RPE as noted by an international panel of SDOCT experts.<sup>32</sup> In addition, the average thickness of the BM is 1 to 5 μm, whereas the axial resolution of the Spectralis SD-OCT machine is 7 μm, making it hard to reliably discern BMO in SD-OCT images. Therefore, the termination of the RPE/BM complex may be a more reliable descriptor of the neuroretinal rim border seen in SD-OCT imaging. The MDB neuroretinal rim parameter is thus defined as the shortest distance between the ILM and the termination of the RPE/BM complex (Fig. 1).<sup>28-30,33</sup> Another fundamental difference between the MDB and the BMO-MRW lies in the image acquisition protocol. The MDB thickness is calculated from high-density raster scans comprised of 193 B-scans resulting in 100 calculated points along the disc border, whereas the BMO-MRW uses lower density radial scans comprised of 24 B-scans, resulting in 48 calculated points along the disc border. In addition, the high-density raster scan protocol allows for the generation of multiple measurements from a single scan, including rim thickness, rim area, and rim volume.<sup>28-30,33</sup> In contrast to the macular region where only 50% of retinal ganglion cells (RGC) reside, 100% of RGC axons must pass through the neuroretinal rim and they account for almost all the tissue in this MDB region (ie, 94% nerve axons and 5% astrocytes).<sup>34</sup> As the MDB measures the minimum space

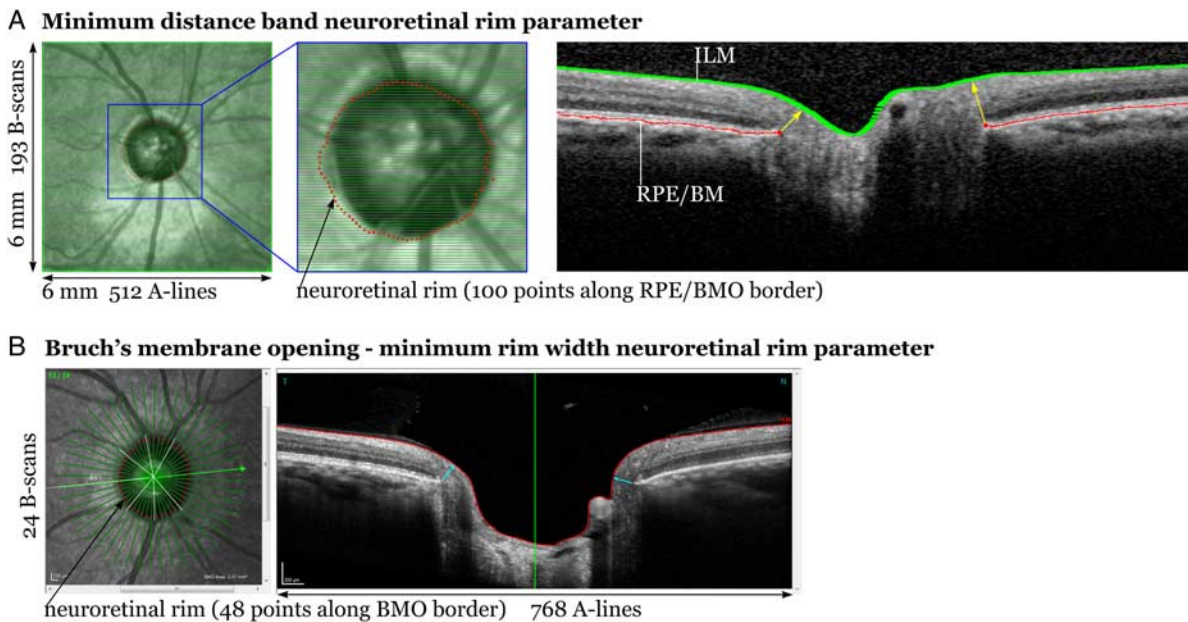


**FIGURE 1.** The neuroretinal rim minimum distance band (MDB) high-density raster scan protocol compared with the Bruch membrane opening-minimum rim width (BMO-MRW) radial scan protocol. A, MDB thickness scan of a glaucomatous eye not included in this study. Each of the horizontal green lines represents 1 of the 193 raster scans (top left), which are then used to reconstruct the neuroretinal rim through 100 points (red dots, top center), defined as the termination of the retinal pigment epithelium/Bruch membrane (RPE/BM) complex. The last image (right right) shows 1 of the 193 B-scans, with the termination of the retinal pigment epithelium/Bruch membrane (RPE/BM) complex delineated in red, and the internal limiting membrane (ILM) in green. The shortest distance between the ILM and the RPE/BM complex is represented by the yellow arrow, although the final average MDB thickness is calculated from a 100-point 3-dimensional reconstruction of the ILM and RPE/BM complex terminations. B, BMO-MRW scan of a healthy eye. Each green line represents 1 of the 24 radial scans used to reconstruct the disc margin at 48 points (red dots, bottom left), which is defined as the border of the BMO. A cross-section at one of those points is shown (bottom right), with the ILM marked by a red line, and the BMO by a red dot, while a blue arrow delineates the BMO-MRW.

through which this trajectory of nerve axons must travel to reach the brain, the MDB is a good surrogate measurement of neuroretinal rim tissue<sup>28,29,33</sup> and affords a good model to assess to effects of age, race, and sex on optic nerve tissue.

To the best of our knowledge, the effects of age, race, and sex on the high-density neuroretinal MDB parameter have not yet been reported. The aim of this study was to determine the relationships between these variables and MDB thickness in a multiethnic population using 3D high-density volume scans acquired by the Spectralis SD-OCT machine (Heidelberg Engineering GmbH, Heidelberg, Germany).

## METHODS

### Participants and Associated Testing

All subjects were recruited from the Glaucoma Service at the Massachusetts Eye and Ear Infirmary between April 2009 and January 2016, though all were deemed to have no glaucomatous damage. This prospective study protocol was approved by the Massachusetts Eye and Ear Infirmary Institutional Review Board, and informed consent and Health Insurance Portability and Accountability Act (HIPAA) forms were signed by all study participants. This study is a cross-sectional sampling of this prospective study. All subjects underwent a complete eye examination by a glaucoma specialist (T.C.C.), which included history, best-corrected visual acuity testing, Goldmann applanation tonometry, slit-lamp biomicroscopy, gonioscopy, ultrasonic pachymetry (PachPen; Accutome Ultrasound Inc., Malvern, PA), dilated ophthalmoscopy, stereo disc photography (Visucam Pro NM; Carl Zeiss Meditec Inc.), VF testing (Swedish Interactive Threshold Algorithm 24-2 test of the Humphrey visual field analyzer 750i; Carl Zeiss Meditec Inc.), as well as RNFL thickness scans (HRA/Spectralis software version 5.4.8.0; Heidelberg Engineering GmbH).

Patients were only included if their VF tests were reliable: <33% fixation losses, <20% false positives, and <20% false negatives; if their RNFL scans had a clear fundus image with good optic disc and scan circle visibility before and during image acquisition, RNFL visible and without interruptions, and a continuous scan pattern without missing or blank areas. All included study patients had normal eyes except for mild cataracts, had best-corrected visual acuities of 20/40 or better, had spherical equivalent refractions within  $\pm 5.0$  D, had intraocular pressures <21 mm Hg and had normal VF testing with normal Glaucoma Hemifield Tests. Normal VF tests did not have a cluster of 3 > -5 dB abnormal spots on the same side of the horizontal meridian and did not have a cluster of -5 and > -10 dB abnormal spots on the same side of the horizontal meridian on the pattern SD map. Although all patients had normal optic nerves, these normal patients were divided into 2 subgroups based on their cup to disc ratios (CDR), which were determined by subjective assessments by a glaucoma specialist (T.C.C.): Subgroup A with normal nerves and subgroup B with normal disc variations (ie, physiologic cupping). Physiologic cupping was defined as having CDR > 0.4 for whites and Asians and > 0.6 for African Americans and Hispanics, with normal VF test results and intraocular pressure <21 mm Hg. Patients were excluded if they had a CDR asymmetry > 0.2, or if scans had a manufacturer signal strength  $\leq 15$  dB. When 2 eyes of the same patient were eligible for the study, 1 eye was randomly selected by the investigator using a random number generator.

### Spectralis SD-OCT Optic Nerve Volume Scan and MDB Calculations

SD-OCT optic nerve volume scans were performed after pupillary dilation using the Spectralis OCT machine, which relies on an 870-nm superluminescent diode source. The Spectralis OCT's automatic real-time function and eye-tracking system were used to increase image quality. The high-density 3D optic nerve head (ONH) volume scan protocol consists of 193 B-scans in a raster pattern over an area 20 degrees by 20 degrees (~6 mm $\times$ 6 mm, depending on the patient's refraction) centered on the ONH. To analyze this volumetric dataset, custom-designed software was written, using C++ with OpenCV, ITK, and VTK libraries (E.T.). The algorithm automatically segments B-scans to reconstruct the ILM and RPE/BM in 3D. Segmentation errors were identified manually and automatically interpolated by the software. The neuroretinal rim was determined from the termination of the RPE/BM complex at 100 circumferential points, and the MDB thickness was calculated by measuring the closest distances from these points to the ILM (Fig. 1). All calculations were performed in real space, though the images in Figure 1 are stretched by a factor of 3 for display purposes. Two adjacent points on the neuroretinal rim and their closest points on the ILM formed pairs of triangles. The MDB area was calculated by measuring the area of the triangle pairs around the rim. Global, quadrant, and octant averages of the thickness and area measurements were determined via the arithmetic mean. Further details of this MDB program have been described in previous studies.<sup>28,29</sup>

### Calculation of Percentage of MDB Thinning Per Year

We calculated the percentage of nerve tissue loss per year for MDB thickness to better compare our results to those of other neuroretinal rim or RNFL thickness parameters, whose normal thickness values may have different magnitudes. The annual percentage of MDB loss was defined as annual MDB thinning (ie, numerator) divided by normal mean MDB thickness measurements (ie, denominator).

### Statistical Analysis

A  $\chi^2$  test was used to test whether the race and sex distributions of the 2 subgroups were different. Simple linear regression analysis was performed to determine the association between age and MDB thickness. A *t* test was used to determine the effect of sex on MDB thickness, and to compare the MDB thickness of the normal subgroup A with that of subgroup B with normal disc variations. An *F* test was performed to determine whether the MDB thickness was different among different races. A Benjamini-Hochberg false discovery rate correction was performed to account for multiple testing of the univariate analyses among all subgroups A and B participants. Furthermore, a multivariate linear regression analysis of MDB thickness was performed, adjusting for age, race, and sex. *P*-values < 0.05 were considered statistically significant. Results are shown as the mean  $\pm$  SD unless otherwise stated. Finally, an analysis of variance *F* test was used to determine whether age-related MDB thickness changes were different across the races included in this study.

## RESULTS

### Subject Characteristics

The study included 256 normal patients: 132 patients in subgroup A with normal discs and 124 patients in subgroup B with normal disc variations (ie, physiologic cupping). The mean

**TABLE 1.** Demographics of Normal Study Population (N=256)

	n (%)			P*
	Overall Normal Study Group	Subgroup A: Normal Discs	Subgroup B: Normal Disc Variations	
Age (mean ± SD) (y)	58.4 ± 15.3	56.8 ± 16.3	60.0 ± 14.0	0.093
Sex				0.346
Female	145 (57)	79 (60)	66 (53)	
Male	111 (43)	53 (40)	58 (47)	
Race				0.004*
White	177 (69)	86 (65)	91 (73)	0.197
African American	31 (12)	21 (16)	10 (8)	0.083
Asian	28 (11)	11 (8)	17 (14)	0.239
Hispanic	17 (7)	14 (11)	3 (2)	0.017*
Other	3 (1)	0	3 (2)	NA
Refractive error (mean ± SD) (D)	-0.66 ± 1.91	-0.40 ± 1.79	-0.94 ± 2.01	0.025*
Overall	256	132	124	

P is the P-value of testing that the proportion of subjects from each demographic is the same in subgroups A and B, measured with a  $\chi^2$  test for sex and race, and the P-value of testing that the means of age and refractive error among subgroups A and B are equal using a t test.  
 NA indicates not available.  
 \*P < 0.05, statistically significant.

age for all 256 patients was 58.4 ± 15.3 years (Table 1). The study population was predominantly female (57%) and white (69%) and included 134 right eyes and 122 left eyes (Table 1).

**MDB Thickness Measurements**

The mean MDB thickness was 278.4 ± 47.5  $\mu$ m for all subjects (Table 2). Most normal eyes did not follow the ISNT rule, which states that the inferior rim is the thickest, followed by the superior rim, the nasal rim, and then the temporal rim as the thinnest.<sup>35</sup> In the overall normal group of 256 patients, only 71 (28%) of 256 eyes obeyed the ISNT rule. Of the normal subgroups, the ISNT rule was only valid for 40 (30%) of 132 eyes of normal subgroup A and 31 (25%) of 124 eyes of subgroup B with normal disc variations. In contrast, the mean MDB thickness values, averaged as an entire group, did follow the ISNT rule (Table 2). Global MDB was thicker in subgroup A with normal discs (302.5 ± 42.2  $\mu$ m) compared with subgroup B (252.7 ± 38.4  $\mu$ m) and across all quadrants and sectors (P < 0.001, Table 3).

**Association of Age and MDB Thickness Measurements**

MDB thickness decreased significantly with age for the overall normal population (P = 0.003), at a rate of 0.71 ± 0.19  $\mu$ m per year (Table 4). The inferior, superior, and nasal quadrants displayed similar results (P < 0.011), whereas temporal MDB thickness did not show a significant correlation with age (P = 0.077, Table 4). Figure 2 shows the decline of MDB thickness with increasing age in the overall normal study population. Results were similar in normal subgroup A with normal discs, whereas subgroup B with normal disc variations did not show a significant decline with age (P = 0.955, Table 4).

**Association of Sex and MDB Thickness Measurements**

There was no difference in MDB thickness between males and females in the overall study population or in either subgroup, globally or in any quadrant or sector (P > 0.162, Table 5).

**TABLE 2.** Neuroretinal Rim MDB Thickness and Area in the Normal Study Population (n = 256) by Quadrant and Sector

	Mean ± SD (95% CI)	
	MDB Thickness ( $\mu$ m)	MDB Area (mm <sup>2</sup> )
Global	278.4 ± 47.5 (272.6-284.2)	1.824 ± 0.409 (1.774-1.874)
Inferior quadrant	312.8 ± 60.6 (305.4-320.2)	0.526 ± 0.142 (0.509-0.543)
Superior quadrant	297.8 ± 62.4 (290.2-305.5)	0.505 ± 0.153 (0.487-0.524)
Nasal quadrant	281.5 ± 56.9 (274.6-288.5)	0.461 ± 0.144 (0.444-0.479)
Temporal quadrant	222.4 ± 47.6 (216.6-228.2)	0.332 ± 0.105 (0.319-0.345)
Inferior nasal sector	325.8 ± 63.3 (318.0-333.5)	0.278 ± 0.080 (0.268-0.288)
Inferotemporal sector	299.8 ± 68.9 (291.3-308.2)	0.248 ± 0.086 (0.238-0.259)
Superior nasal sector	304.4 ± 66.7 (296.2-312.5)	0.254 ± 0.090 (0.243-0.265)
Superotemporal sector	298.0 ± 63.9 (290.2-305.9)	0.252 ± 0.086 (0.241-0.262)

CI indicates confidence interval; MDB, minimum distance band.

**TABLE 3.** Neuroretinal Rim MDB in the Normal Subgroup A (Normal Discs, n = 132) and Normal Subgroup B (Normal Disc Variations, n = 124), by Quadrant and Sector

	MDB Thickness [Mean ± SD (95% CI)] (µm)		
	Subgroup A:	Subgroup B:	P*
	Normal Discs (n = 132)	Normal Disc Variations (n = 124)	
Global	302.5 ± 42.2 (295.2-309.7)	252.7 ± 38.4 (246.0-259.5)	< 0.001*
Inferior quadrant	337.2 ± 57.3 (327.4-346.9)	286.9 ± 53.0 (277.5-296.2)	< 0.001*
Superior quadrant	328.7 ± 54.0 (319.5-337.9)	265.0 ± 53.6 (255.5-274.4)	< 0.001*
Nasal quadrant	304.6 ± 53.2 (295.5-313.7)	257.0 ± 50.2 (248.1-265.8)	< 0.001*
Temporal quadrant	240.5 ± 44.8 (232.9-248.2)	203.1 ± 42.8 (195.5-210.6)	< 0.001*
Inferior nasal sector	348.5 ± 62.4 (337.9-359.2)	301.6 ± 54.9 (291.9-311.2)	< 0.001*
Inferotemporal sector	325.4 ± 61.6 (314.9-335.9)	272.4 ± 65.9 (260.8-284.0)	< 0.001*
Superior nasal sector	336.2 ± 59.0 (326.1-346.3)	270.5 ± 57.1 (260.4-280.5)	< 0.001*
Superotemporal sector	328.2 ± 52.9 (319.2-337.2)	265.9 ± 59.0 (255.5-276.3)	< 0.001*

P is the chance that the MDB thickness is equal in subgroups A and B. A false discovery rate correction was applied to all calculations. CI indicates confidence interval; MDB, minimum distance band. \*P < 0.05, statistically significant.

**Association of Race and MDB Thickness Measurements**

Mean MDB thickness was highest among Hispanics (286.2 ± 57.7 µm), followed by whites (283.7 ± 44.0 µm), Asians (269.5 ± 40.1 µm), and African Americans (258.6 ± 57.5 µm) (P = 0.011, Table 6). African Americans had the thinnest global, temporal, and inferior nasal MDB, whereas Asians had the thinnest nasal MDB, and Hispanics had the thickest MDB in all 4 regions. P-values for testing of mean equality of MDB measurements across races were P = 0.011, 0.008, 0.026, 0.006 for global, temporal, inferior nasal, and nasal sections. MDB thickness in other quadrants and sectors was similar between all 4 races (P > 0.051, Table 6).

**Changes in MDB Thickness Adjusted for Age, Race, and Sex**

A multivariate analysis was performed on MDB thickness in the overall study group (n = 256), adjusted for age, race using whites as a reference group, and sex using females as a reference group. The MDB thickness decreased globally (0.84 ± 0.19 µm/year, P < 0.001), and across all quadrants and sectors with age

(P < 0.014, Table 7) at a higher rate after adjusting for race and sex. African Americans had thinner MDB than whites globally (P = 0.003) and across the inferior, nasal, and temporal quadrants, and the inferonasal and superior temporal sectors (P = 0.003, 0.028, 0.010, < 0.001, 0.013, and 0.043, respectively), whereas the superior quadrant, superonasal and inferotemporal sectors were similar among African Americans and whites (P = 0.095, 0.434, and 0.111, respectively). Asians also had significantly thinner MDB compared with whites in the global, nasal, and inferonasal measurements (P = 0.031, < 0.001, and 0.032, respectively). Hispanics had similar MDB thickness to whites globally (P = 0.826) and across all quadrants and sectors (P > 0.225). After adjusting for age and race, males and females had similar MDB thickness globally and in all quadrants and sectors (P > 0.050) except the superotemporal sector, where males had thinner MDB (P = 0.045). Age-related MDB thinning was not significantly different across all races (P > 0.235).

**MDB Area Measurements**

The mean MDB area in the study population was 1.824 ± 0.409 mm<sup>2</sup> and overall average group values for the

**TABLE 4.** Effect of Age on Neuroretinal Rim MDB Thickness in the Normal Study Population (n = 256), the Normal Subgroup A (n = 132), and the Normal Subgroup B With Normal Disc Variations (n = 124), by Quadrant and Sector

	Overall Normal Study Group (n = 256)		Subgroup A: Normal Discs (n = 132)		Subgroup B: Normal Disc Variations (n = 124)	
	MDB Thinning Per Year (Mean ± SD) (µm)	P*	MDB Thinning Per Year (Mean ± SD) (µm)	P*	MDB Thinning Per Year (µm)	P*
Global	0.71 ± 0.19	0.003*	0.81 ± 0.22	0.003*	0.14	0.955
Inferior quadrant	0.81 ± 0.24	0.006*	1.04 ± 0.30	0.003*	0.06	0.955
Superior quadrant	0.75 ± 0.25	0.011*	0.80 ± 0.28	0.021*	0.15	0.955
Nasal quadrant	0.87 ± 0.23	0.003*	1.02 ± 0.27	0.003*	0.25	0.955
Temporal quadrant	0.41 ± 0.19	0.077	0.39 ± 0.24	0.266	0.12	0.955
Inferior nasal sector	0.74 ± 0.26	0.011*	0.93 ± 0.33	0.021*	0.09	0.955
Inferotemporal sector	0.87 ± 0.28	0.003*	1.15 ± 0.32	0.027*	0.03	0.955
Superior nasal sector	0.97 ± 0.27	0.008*	1.13 ± 0.30	0.025*	0.21	0.955
Superotemporal sector	0.52 ± 0.26	0.088	0.51 ± 0.28	0.211	0.02	0.955

Calculations were performed using a univariate analysis model. P is the chance that the change due to age is not statistically different from a slope of 0, indicating no change due to age. A false discovery rate correction was applied to all calculations. MDB indicates minimum distance band. \*P < 0.05, statistically significant.

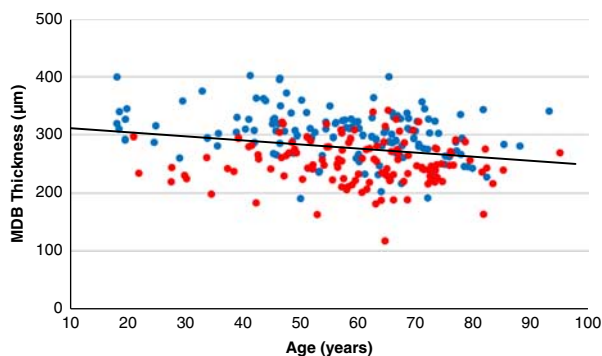


**FIGURE 2.** Scatter-plot showing the relationship between age (y) and the total mean neuroretinal rim minimum distance band (MDB) thickness ( $\mu\text{m}$ ) in the normal study population ( $n=256$ ). Increasing age was significantly associated with decreasing MDB thickness ( $P < 0.001$ ). Subgroup A with normal discs is shown in blue, subgroup B with normal disc variations is shown in red.

MDB area followed the ISNT rule (Table 2). In the normal subgroup A, the mean MDB area was  $1.975 \pm 0.410 \text{ mm}^2$ . The superior and inferior quadrants were similar in size ( $0.564 \pm 0.148$  and  $0.562 \pm 0.137 \text{ mm}^2$ , respectively), followed by the nasal ( $0.493 \pm 0.144 \text{ mm}^2$ ) and temporal quadrants ( $0.357 \pm 0.116 \text{ mm}^2$ ). In subgroup B with normal disc variations, the global MDB area was  $1.664 \pm 0.342 \text{ mm}^2$ . The average subgroup quadrant values followed the ISNT rule ( $0.487 \pm 0.137$ ,  $0.443 \pm 0.132$ ,  $0.428 \pm 0.137$ , and  $0.305 \pm 0.084 \text{ mm}^2$ , respectively).

**DISCUSSION**

To our knowledge, this is the first study that describes the relationship of age, race, and sex with the 3D SD-OCT MDB neuroretinal rim parameter. On average, global MDB thickness decreases  $0.84 \pm 0.19 \mu\text{m}$  per year (Table 7), with similar rates between men and women ( $P > 0.162$ , Table 5). In terms of ethnic differences, African Americans had

significantly thinner MDB values compared with whites ( $258.6 \pm 57.5$  vs.  $283.7 \pm 44.0 \mu\text{m}$ ,  $P = 0.003$ ). Although differences were not significant, Hispanics had larger global MDB thickness values ( $286.2 \pm 57.7 \mu\text{m}$ ) and Asians had thinner MDB values ( $269.5 \pm 40.1$ ) compared with whites (Table 6). Since neuroretinal rim thickness measurements such as the MDB thickness and BMO-MRW may be considered diagnostically superior to area measurements, such as MDB area or BMO area, this paper’s discussion focuses on the MDB thickness.<sup>30,33,36</sup>

Like RNFL thickness measurements, MDB neuroretinal rim thickness also decreases with age (Tables 4, 7, 8). Age-related RNFL thinning has been reported to be  $0.18$  to  $0.44 \mu\text{m}$  per year as measured by SD-OCT.<sup>10–12,17–20,37</sup> As RNFL and MDB measure different anatomic regions and therefore have different normal mean values, comparing rates of percentage decline instead of absolute value decline would make a comparison of these 2 parameters easier. Therefore, past cross-sectional studies have reported that annual RNFL thinning ranges between  $0.15\%$  by Alasil and colleagues to  $0.38\%$  by Celebi and colleagues.<sup>12,17–20,37</sup> Vianna et al<sup>11</sup> reported a decline of  $0.46\%$  per year in 37 normal adults over the course of a 4-year (range: 2 to 6 y) longitudinal study. To compare MDB thickness to RNFL thickness and BMO-MRW, we converted the annual decline measured in microns into a proportion and presented it in Table 8. The MDB thickness decreased by an average annual rate of  $0.25\%$  in our 256 normal study subjects, indicating that our results on the MDB age-related thinning are in line with the existing literature on RNFL age-related thinning (Table 8).

Rates for age-related decline of the BMO-MRW neuroretinal rim parameter have been reported at  $1.34$  to  $1.92 \mu\text{m}$  per year, similar to the MDB thinning of  $0.84 \mu\text{m}$  per year reported in this study (Table 7).<sup>11,12,19</sup> When using the same methodology as the current study to calculate rates of percentage decline, BMO-MRW studies reported a decline of  $0.40\%$  to  $0.63\%$  per year, which is higher but similar to the  $0.25\%$  decline reported in this study for global MDB thickness (Table 8).<sup>11,12,19</sup> In a confocal scanning laser tomography (CSLT) study, Enders et al<sup>38</sup> more recently reported a decline of  $0.80 \mu\text{m}$  per year (or  $0.34\%$ /year) in adults with a large ONH, defined as having an area  $\geq 2.45 \text{ mm}^2$ . This rate of  $0.34\%$  per year by CSLT is similar to the rate of  $0.30\%$  per year by SD-OCT in this study (Tables 7, 8). One reason for the slight difference between percentage decline for the BMO-MRW parameter ( $0.40\%$  to  $0.63\%$ /year)<sup>11,12,19</sup> and the MDB thickness parameter ( $0.30\%$ /year, Tables 7, 8) may be that the BMO-MRW and MDB thickness measurements are procured differently. For example, the BMO-MRW low-density scan protocol consists of 24 radial scans, with 25 averages each, whereas the MDB parameter is derived from a high-density 3D volume scan with 193 raster lines, with 3 averages each.<sup>28,29</sup> The definition of the disc border also differs between the BMO-MRW and the MDB thickness parameter, because the BMO is used for the BMO-MRW parameter and the termination of the RPE/BM complex is used for the MDB parameter. These data acquisition differences may have accounted for the slight difference between BMO-MRW and MDB rates of age-related decline. Nevertheless, this study and the past literature overall seems to suggest that neuroretinal rim parameters by CSLT and SD-OCT appear to have similar percentage rates of decline.

Rates of age-related neuroretinal thinning as measured by SD-OCT in this study are similar to those reported in past

**TABLE 5.** Effect of Sex on Neuroretinal Rim MDB Thickness in the Normal Study Population ( $n=256$ ), by Quadrant and Sector

	MDB Thickness (Mean $\pm$ SD) ( $\mu\text{m}$ )		P*
	Females	Males	
Global	279.5 $\pm$ 48.2	276.9 $\pm$ 46.7	0.790
Inferior quadrant	313.9 $\pm$ 63.6	311.3 $\pm$ 56.7	0.819
Superior quadrant	302.1 $\pm$ 62.5	292.2 $\pm$ 62.2	0.299
Nasal quadrant	281.0 $\pm$ 59.0	282.2 $\pm$ 54.3	0.897
Temporal quadrant	222.2 $\pm$ 46.0	222.6 $\pm$ 49.9	0.946
Inferior nasal sector	326.7 $\pm$ 64.2	324.6 $\pm$ 62.3	0.856
Inferotemporal sector	301.4 $\pm$ 74.4	297.7 $\pm$ 61.6	0.790
Superior nasal sector	308.9 $\pm$ 66.1	298.4 $\pm$ 67.2	0.299
Superotemporal sector	303.8 $\pm$ 63.0	290.6 $\pm$ 64.7	0.162

Calculations were performed using a univariate analysis model.  
 P is the chance that the difference between mean MDB measurements of males and females is not statistically different from a slope of 0, indicating no difference. A false discovery rate correction was applied to all calculations.  
 MDB indicates minimum distance band.  
 \* $P < 0.05$ , statistically significant.

**TABLE 6.** Effect of Race on Neuroretinal Rim MDB Thickness in the Normal Study Population (n = 256), by Quadrant and Sector

	MDB Neuroretinal Rim Thickness (µm)				P*
	White	African American	Asian	Hispanic	
No. subjects	177	31	28	17	
Global	283.7 ± 44.0	258.6 ± 57.5	269.5 ± 40.1	286.2 ± 57.7	0.011*
Inferior quadrant	317.7 ± 58.3	293.7 ± 67.4	304.8 ± 50.7	320.2 ± 77.3	0.144
Superior quadrant	300.3 ± 59.2	283.5 ± 75.1	295.1 ± 60.0	316.2 ± 69.9	0.144
Nasal quadrant	289.7 ± 53.3	264.9 ± 62.2	258.9 ± 58.0	280.0 ± 60.1	0.006*
Temporal quadrant	227.8 ± 44.2	193.4 ± 52.9	220.9 ± 48.4	229.0 ± 52.3	0.008*
Inferior nasal sector	332.7 ± 59.7	304.3 ± 68.8	312.2 ± 49.2	330.6 ± 90.2	0.026*
Inferotemporal sector	302.8 ± 68.5	282.8 ± 74.2	309.3 ± 68.0	309.3 ± 68.0	0.615
Superior nasal sector	306.0 ± 61.7	296.1 ± 79.9	303.6 ± 74.8	317.9 ± 77.0	0.342
Superotemporal sector	301.8 ± 60.2	276.0 ± 78.5	295.5 ± 60.6	318.0 ± 68.0	0.051

Results are expressed as mean ± SD.

Calculations performed using a univariate analysis model.

P is the chance that the MDB thickness is the same across all races, measured with an F test using analysis of variance. A false discovery rate correction was applied to all calculations.

MDB indicates minimum distance band.

\*P < 0.05, statistically significant.

histologic studies, which have found a significant age-related decline in the number of RGC axons.<sup>39-42</sup> The estimated mean nerve fiber count is around 0.97 to 1.24 million fibers,<sup>40-42</sup> with a mean loss of around 4000 to 5400 fibers (0.32% to 0.54%) per year.<sup>39,41,42</sup> The annual rates of thinning measured in this study, 0.253% for MDB thickness and 0.279% for MDB area (Table 8), are similar to those reported in histologic studies, which confirms the good correlation between neuroretinal MDB OCT measurements and histologic nerve fiber counts. The subtle differences between the predicted decay and the observed decay may be due to the presence of nonaxonal tissue or even blood vessel artifacts which may influence MDB calculations.<sup>33</sup> Although future studies are needed to verify this hypothesis, MDB thickness measurements may better reflect nerve tissue loss compared with RNFL thickness measurements, because the MDB thickness measurements have a higher component of nerve to non-neuronal tissue. For example, primate histology studies indicate the MDB may be comprised of up to 94% nerve axons and only 5% astrocytes,<sup>34</sup>

whereas the RNFL is composed of at least 18% glial cells, including Muller cells and astrocytes.<sup>43</sup> In addition, SD-OCT studies suggest that the RNFL thickness measurements may be comprised of almost 48.8% to 65.1% of non-neuronal tissue (ie, glial cells and blood vessels).<sup>44</sup> Even though SD-OCT RNFL thickness studies have well-substantiated a “floor effect” ranging from 49.2 to 64.7 µm due to glial cells and blood vessels,<sup>28,44</sup> future studies of MDB thickness are needed to verify that the “floor effect” for MDB measurements are indeed lower than that for RNFL thickness measurements. These future studies would further substantiate whether OCT is an accurate form of in vivo histology or not.<sup>45</sup>

Table 4 shows that rates of age-related decline in MDB thickness were similar for all quadrants and sectors except for the temporal quadrant, which did not decline with age (P = 0.077). This is consistent with studies on RNFL age-related thinning, which showed that the thickness of the mean, superior, inferior, and nasal quadrants decreased with age, whereas the temporal quadrant did not.<sup>12,20,37</sup> After adjusting

**TABLE 7.** Effect of Age on Neuroretinal Rim MDB Thickness Adjusted for Race and Sex in the Overall Study Population (n = 256), With Annual Rate of MDB Decline in the Normal Study Population (n = 256), by Quadrant and Sector

	MDB Thinning Per Year (Mean ± SD) (µm)	P*	MDB Thinning Per Year (%)
Global	0.84 ± 0.19	< 0.001*	0.301
Inferior quadrant	0.94 ± 0.25	< 0.001*	0.300
Superior quadrant	0.88 ± 0.26	0.001*	0.291
Nasal quadrant	1.07 ± 0.22	< 0.001*	0.381
Temporal quadrant	0.48 ± 0.19	0.014*	0.216
Inferior nasal sector	0.92 ± 0.26	< 0.001*	0.282
Inferotemporal sector	0.96 ± 0.29	0.001*	0.319
Superior nasal sector	1.11 ± 0.27	< 0.001*	0.359
Superotemporal sector	0.67 ± 0.26	0.012*	0.221

Calculations were performed using a multivariate analysis model, with MDB thickness as the dependent variable, and age, race, and sex as the independent variables.

P is the chance that the change due to age is not statistically different from a slope of 0, indicating no change due to age. A false discovery rate correction was applied to all calculations.

MDB thinning ratio is calculated by dividing the annual rate of MDB thinning (column 1) by the mean MDB thickness in the overall population (Table 2).

MDB indicates minimum distance band.

\*P < 0.05, statistically significant.

**TABLE 8.** Annual Rate of Neuroretinal Rim MDB Decline in the Normal Study Population (n = 256) for Thickness, by Quadrant and Sector

	MDB Thinning Per Year (%)		
	Overall Normal Study Group (n = 256)	Subgroup A: Normal Discs (n = 132)	Subgroup B: Normal Disc Variations (n = 124)
Global	0.253	0.269	0.056
Inferior quadrant	0.258	0.309	0.019
Superior quadrant	0.251	0.243	0.057
Nasal quadrant	0.308	0.337	0.097
Temporal quadrant	0.183	0.163	0.057
Inferior nasal sector	0.228	0.267	0.030
Inferotemporal sector	0.289	0.353	0.010
Superior nasal sector	0.319	0.336	0.076
Superotemporal sector	0.176	0.156	0.008

The annual MDB thinning ratio is calculated by dividing the average thinning with age (Table 4), by the mean MDB thickness (Tables 2, 3), and multiplying by 100.

MDB indicates minimum distance band.

for sex and race, the temporal quadrant declined significantly with age ( $P=0.014$ ), but it had the slowest rate of age-related decline when analyzed for the entire study population compared with other quadrants (ie,  $0.48\ \mu\text{m}$  compared with  $0.88$  to  $1.07\ \mu\text{m}$  yearly, or  $0.18\%$  compared with  $0.25\%$  to  $0.31\%$  yearly, Table 7). This is similar to results in the BMO-MRW, where all quadrants declined with age and the temporal quadrant showed the slowest rate of decline.<sup>12</sup> One possible explanation for the slower rate of age-related decline for the temporal quadrant is that it contains the papillomacular bundle, which is composed of thinner axons.<sup>41</sup> Thus, assuming an equal loss in the number of axons across all quadrants, the temporal quadrant would display the least thinning as it has the thinnest axons to start with. Another theory is that slower axonal loss near the fovea may be an evolutionary protective mechanism to preserve central vision, which is supported by the temporal region of the ONH.<sup>37</sup>

Subjects with normal disc variation (ie, physiologic cupping) had thinner MDB values than those with normal discs ( $P<0.001$ , Table 3) and showed no significant thinning with age ( $P=0.955$ , Table 4), whereas those with normal discs showed significant MDB thinning with age across all but the temporal quadrant and the superotemporal sector ( $P<0.028$ , Table 4). Subgroup B with physiologic cupping was more myopic than subgroup A with normal discs (Table 1), which may affect MDB thickness measurements due to increased optic disc tilt or peripapillary atrophy. Subgroup B also had significantly fewer Hispanics than subgroup A (Table 1), which may have contributed to the thinner MDB measured in subgroup B compared with subgroup A, as Hispanics had the thickest MDB measurements overall (Table 6). The difference in age-related MDB decline among the 2 groups may be due to the fact that subjects with physiologic cupping have a lower mean MDB thickness. The normal variability of subjects within each subgroup may also explain the difference in age-related change, as aging may act differently on certain groups or individuals. In addition, as the main difference between normal subgroup B patients and normal subgroup A patients is the larger CDR of subgroup B, it is likely that this larger CDR may play a role in their having thinner MDBs and their having a smaller percentage decline in neuroretinal rim thickness per year (Table 8). Individuals with a larger CDR sometimes have a larger disc diameter, which means that despite having a similar number of axons, the neuroretinal rim

is expected to be thinner in individuals with a larger CDR. A study by Tatham et al<sup>46</sup> also concluded that small differences in CDR were inversely correlated with large changes in RGC count which in turn affects neuroretinal rim thickness.

In line with previous studies on RNFL thickness, our study showed that sex did not affect MDB thickness measurements ( $P=0.790$ , Table 5).<sup>17,19,20,23,47</sup> Like our current study, the literature is also conflicted on the effect of sex on OCT measurements.<sup>48–50</sup> Tun et al<sup>48</sup> reported a significant relationship between BMO-MRW and sex in a normal Chinese population, with females having thicker measurements.

Table 6 shows that MDB thickness was different among races only in the global, nasal, temporal, and inferior nasal measurements ( $P<0.027$ ). However, no significant difference in age-related MDB thinning was detected across races ( $P>0.235$ ), which may be due to small sample size. A multivariate analysis adjusting for age and sex also showed that African Americans generally have thinner MDB thickness measurements compared with whites globally and across all but the superior quadrant ( $P<0.029$ ). This is consistent with past studies that have noted thinner temporal RNFL thickness values in African Americans.<sup>18,49,51</sup> However, Knight et al<sup>49</sup> reported, compared with whites, African Americans had thicker mean and quadrant RNFL measurements in all but the temporal quadrant, whereas other studies have reported no significant differences in mean global RNFL thickness between African Americans and whites.<sup>18,20,51</sup> Rhodes and colleagues found no significant difference in BMO-MRW thickness between subjects of European descent (ED) and those of African descent (AD), but reported that the RNFL was thinner in AD subjects in the temporal and superior temporal regions and thicker in the nasal, inferotemporal, inferonasal, and superior nasal regions.<sup>51</sup> In a longitudinal study of BMO-MRW and RNFL thickness among AD and ED subjects, Bowd et al<sup>52</sup> found no difference in baseline BMO-MRW, annual BMO-MRW thinning, RNFL thickness, or RNFL thinning in healthy subjects among the 2 groups, although they did note a faster rate of BMO-MRW thinning in AD “glaucoma suspects,” compared with their ED counterparts. Some studies have also found no significant difference in rim area among subjects of different races.<sup>49,53</sup>

Although our study found that MDB thickness values in Hispanics were similar to those of whites ( $P>0.225$ ), it is difficult to say if these results are generalizable, because there were only 17 Hispanic subjects in this study, which



makes it difficult to avoid type II errors. Our study also found that Asians had thinner MDB compared with whites globally, nasally, and inferonasally ( $P < 0.033$ ). Studies on the difference in RNFL thickness between Asians and whites were conflicted.<sup>20,50</sup> Girkin et al<sup>18</sup> studied RNFL thickness among 2 Asian ethnicities, Indians and Japanese, and found no difference between mean global RNFL thickness of Japanese and Indian subjects compared with those of ED or between Japanese and Indian subjects. However, the study found that subjects of Indian descent had thicker RNFL than Europeans across all quadrants, whereas subjects of Japanese descent had thicker nasal RNFL than those of ED, but were similar in all other quadrants.<sup>20</sup> Another study, by Knight et al,<sup>49</sup> noted that Asians had a thicker RNFL than Europeans across all quadrants except the nasal quadrant, which was similar in thickness among both groups. One possible explanation for the existence of racial differences in our study is that Hispanics, Asians, and African Americans are believed to have a larger optic disc size compared with whites.<sup>54</sup> The MDB, which measures neuroretinal rim tissue, may be more affected by disc morphology than the RNFL, leading to differences that are not observed in the RNFL studies. Girkin et al<sup>53</sup> also hypothesized that the lack of a significant effect of race on the diagnostic performance of SD-OCT may be due to individual differences among subjects of the same race, which may exceed the difference between multiple races. Another possible explanation may be the small sample size of nonwhites in our study (Table 1), which makes finding statistically significant differences more difficult. A post hoc power analysis revealed that our study does have sufficient power to test whether MDB thickness differences exist among all groups in the global, nasal, temporal, and inferonasal regions (power > 90%). However, when comparing the 2 largest groups, African Americans and whites, we only had 74% power to detect differences in global thickness, and 97% power to detect differences in the temporal region, with all other regions falling < 65% power. It is important to note that the post hoc power analysis utilized the mean MDB thickness values in the observed sample (Table 6) as the true value during the calculation, which explains why the power is highest in the regions with the largest difference between African Americans and whites.

Our study has several limitations. As with any cross-sectional study which attempts to evaluate the longitudinal effects of aging, our study results may not accurately reflect the real effects of aging, which is best evaluated in a longitudinal study. Nevertheless, this cross-sectional study still provides useful information, because a longitudinal study over many decades is not possible as SD-OCT has only been commercially available for the past decade or so. Future studies are needed with larger sample sizes of all racial subgroups, to better assess if racial differences exist between whites and other groups. No statistically significant difference in age-related decline was detected across races, which can be the result of a small sample size. We performed a power analysis which concluded that with a sample size of 256 participants, equal to the observed sample size, we have 41% power to detect such difference, whereas a sample size of 580 participants, with race proportions equal to the ones in our observed data, is needed to have 80% power. In addition, including a larger range of refractive errors would have enabled us to elucidate the effects of myopia or hyperopia on normal MDB thickness and area measurements. Another possible limitation of the study is the use of the default Spectralis pixel conversions when acquiring the images, which may vary with

refraction. Therefore, a better study design would have corrected for refractive errors before acquiring the scans. Finally, future studies should account for variations in optic disc size, which can affect the size of the RPE/BM termination opening, which in turn may affect MDB neuroretinal rim thickness measurements.

In summary, this study shows that age-related decline in neuroretinal MDB thickness normally occurs at the rate of  $0.71 \pm 0.19 \mu\text{m}$  each year (Table 4), which increases to  $0.84 \pm 0.19$  (Table 7) when adjusted for race and sex. Sex does not appear to affect MDB thickness measurements ( $P > 0.162$ , Table 5). African Americans and Asians had thinner MDB neuroretinal rims compared with whites ( $P = 0.003$  and  $0.031$ , respectively), whereas MDB thickness measurements for Hispanics were statistically similar to those of whites ( $P = 0.826$ ). We believe that the results of this study can better inform clinicians on how to account for the effect of normal aging when analyzing MDB thickness measurements over the years.

## REFERENCES

1. Quigley HA, Dunkelberger GR, Green WR. Retinal ganglion cell atrophy correlated with automated perimetry in human eyes with glaucoma. *Am J Ophthalmol.* 1989;107:453–464.
2. Wojtkowski M, Leitgeb R, Kowalczyk A, et al. In vivo human retinal imaging by Fourier domain optical coherence tomography. *J Biomed Opt.* 2002;7:457–463.
3. Wu H, de Boer JF, Chen TC. Reproducibility of retinal nerve fiber layer thickness measurements using spectral domain optical coherence tomography. *J Glaucoma.* 2011;20:470–476.
4. Wu H, de Boer JF, Chen TC. Diagnostic capability of spectral-domain optical coherence tomography for glaucoma. *Am J Ophthalmol.* 2012;153:815.e2–826.e2.
5. Mwanza JC, Oakley JD, Budenz DL, et al. Cirrus Optical Coherence Tomography Normative Database Study Group. Ability of cirrus HD-OCT optic nerve head parameters to discriminate normal from glaucomatous eyes. *Ophthalmology.* 2011;118:241.e1–248.e1.
6. Mwanza JC, Budenz DL, Godfrey DG, et al. Diagnostic performance of optical coherence tomography ganglion cell—inner plexiform layer thickness measurements in early glaucoma. *Ophthalmology.* 2014;121:849–854.
7. Na JH, Sung KR, Baek S, et al. Macular and retinal nerve fiber layer thickness: which is more helpful in the diagnosis of glaucoma? *Invest Ophthalmol Vis Sci.* 2011;52:8094–8101.
8. Schulze A, Lamparter J, Pfeiffer N, et al. Diagnostic ability of retinal ganglion cell complex, retinal nerve fiber layer, and optic nerve head measurements by Fourier-domain optical coherence tomography. *Graefes Arch Clin Exp Ophthalmol.* 2011;249:1039–1045.
9. Chen TC, Cense B, Pierce MC, et al. Spectral domain optical coherence tomography: ultrahigh-speed, ultrahigh-resolution ophthalmic imaging. *Arch Ophthalmol.* 2005;123:1715–1720.
10. Holló G, Zhou Q. Evaluation of retinal nerve fiber layer thickness and ganglion cell complex progression rate in healthy, ocular hypertensive, and glaucoma eyes with the Avanti RTVue-XR optical coherence tomograph based on 5-year follow-up. *J Glaucoma.* 2016;25:e905–e909.
11. Vianna JR, Dhanurebandara VM, Sharpe GP, et al. Importance of normal aging in estimating the rate of glaucomatous neuroretinal rim and retinal nerve fiber layer loss. *Ophthalmology.* 2015;122:2392–2398.
12. Chauhan BC, Dhanurebandara VM, Sharpe GP, et al. Bruch's membrane opening minimum rim width and retinal nerve fiber layer thickness in a normal white population: a multicenter study. *Ophthalmology.* 2015;22:1786–1794.
13. Quigley HA, Addicks EM, Green WR. Optic nerve damage in human glaucoma. III. Quantitative correlation of nerve fiber loss and visual field defect in glaucoma, ischemic neuropathy, papilledema, and toxic neuropathy. *Arch Ophthalmol.* 1982;100:135–146.

14. Johnson CA, Sample PA, Zangwill LM, et al. Structure and function evaluation (SAFE): II. Comparison of optic disk and visual field characteristics. *Am J Ophthalmol*. 2003;135:148–154.
15. Sommer A, Katz J, Quigley HA, et al. Clinically detectable nerve fiber atrophy precedes the onset of glaucomatous field loss. *Arch Ophthalmol*. 1991;109:77–83.
16. Turalba AV, Grosskreutz C. A review of current technology used in evaluating visual function in glaucoma. *Semin Ophthalmol*. 2010;25:309–316.
17. Celebi AR, Mirza GE. Age-related change in retinal nerve fiber layer thickness measured with spectral domain optical coherence tomography. *Invest Ophthalmol Vis Sci*. 2013;54:8095–8103.
18. Girkin CA, McGwin G Jr, Sinai MJ, et al. Variation in optic nerve and macular structure with age and race with spectral domain optical coherence tomography. *Ophthalmology*. 2011;118:2403–2408.
19. Patel NB, Lim M, Gajjar A, et al. Age associated changes in the retinal nerve fiber layer and optic nerve head. *Invest Ophthalmol Vis Sci*. 2014;55:5134–5143.
20. Alasil T, Wang K, Keane PA, et al. Analysis of normal retinal nerve fiber layer thickness by age, sex, and race using spectral domain optical coherence tomography. *J Glaucoma*. 2013;122:532–541.
21. Demirkaya N, van Dijk HW, van Schuppen SM, et al. Effect of age on individual retinal layer thickness in normal eyes as measured with spectral-domain optical coherence tomography. *Invest Ophthalmol Vis Sci*. 2013;54:4934–4940.
22. Bendschneider D, Tornow RP, Horn FK, et al. Retinal nerve fiber layer thickness in normals measured by spectral domain OCT. *J Glaucoma*. 2010;19:475–482.
23. Rao HL, Kumar AU, Babu JG, et al. Predictors of normal optic nerve head, retinal nerve fiber layer, and macular parameters measured by spectral domain optical coherence tomography. *Invest Ophthalmol Vis Sci*. 2011;52:1103–1110.
24. Wang YX, Pan Z, Zhao L, et al. Retinal nerve fiber layer thickness. The Beijing Eye Study 2011. *PLoS One*. 2013;8:e66763.
25. Liu Y, Simavli H, Que CJ, et al. Patient characteristics associated with artifacts in Spectralis optical coherence tomography imaging of the retinal nerve fiber layer in glaucoma. *Am J Ophthalmol*. 2015;159:565.e2–576.e2.
26. Asrani S, Essaid L, Alder BD, et al. Artifacts in spectral-domain optical coherence tomography measurements in glaucoma. *JAMA Ophthalmol*. 2014;132:396–402.
27. Reis AS, Sharpe GP, Yang H, et al. Optic disc margin anatomy in subjects with glaucoma and normal controls with spectral domain optical coherence tomography. *Ophthalmology*. 2012;119:738–747.
28. Tsikata E, Lee R, Shieh E, et al. Comprehensive three-dimensional analysis of the neuroretinal rim in glaucoma using high-density spectral-domain optical coherence tomography volume scans. *Invest Ophthalmol Vis Sci*. 2016;57:5498–5508.
29. Shieh E, Lee R, Que C, et al. Diagnostic performance of a novel three-dimensional neuroretinal rim parameter for glaucoma using high-density volume scans. *Am J Ophthalmol*. 2016;169:168–178.
30. Fan KC, Tsikata E, Khoueir Z, et al. Enhanced diagnostic capability for glaucoma of 3-dimensional versus 2-dimensional neuroretinal rim parameters using spectral domain optical coherence tomography. *J Glaucoma*. 2017;26:450–458.
31. Povazay B, Hofer B, Hermann B, et al. Minimum distance mapping using three-dimensional optical coherence tomography for glaucoma diagnosis. *J Biomed Opt*. 2007;12:041204.
32. Staurengi G, Satta S, Chakravarthy U, et al. Proposed lexicon for anatomic landmarks in normal posterior segment spectral-domain optical coherence tomography: the IN OCT consensus. *Ophthalmology*. 2014;121:1572–1578.
33. Chen TC. Spectral domain optical coherence tomography in glaucoma: qualitative and quantitative analysis of the optic nerve head and retinal nerve fiber layer (an AOS thesis). *Trans Am Ophthalmol Soc*. 2009;107:254–281.
34. Minckler DS, McLean IW, Tso MO. Distribution of axonal and glial elements in the rhesus optic nerve head studied by electron microscopy. *Am J Ophthalmol*. 1976;82:179–187.
35. Jonas JB, Gusek GC, Naumann GO. Optic disc, cup and neuroretinal rim size, configuration and correlations in normal eyes. *Invest Ophthalmol Vis Sci*. 1988;29:1151–1158.
36. Fortune B, Hardin C, Reynaud J, et al. Comparing optic nerve head rim width, rim area, and peripapillary retinal nerve fiber layer thickness to axon count in experimental glaucoma. *Invest Ophthalmol Vis Sci*. 2016;57:OCT404–OCT412.
37. Sung KR, Wollstein G, Bilonick RA, et al. Effects of age on optical coherence tomography measurements of healthy retinal nerve fiber layer, macula, and optic nerve head. *Ophthalmology*. 2009;116:1119–1124.
38. Enders P, Schaub F, Hermann MM, et al. Neuroretinal rim in non-glaucomatous large optic nerve heads: a comparison of confocal scanning laser tomography and spectral domain optical coherence tomography. *Br J Ophthalmol*. 2017;101:138–142.
39. Jonas JB, Schmidt AM, Muller Bergh JA, et al. Human optic nerve fiber count and optic disc size. *Invest Ophthalmol Vis Sci*. 1992;33:2012–2018.
40. Balazsi AG, Rootman J, Drance SM, et al. The effect of age on the nerve fiber population of the human optic nerve. *Am J Ophthalmol*. 1984;97:760–766.
41. Mikelberg FS, Drance SM, Schulzer M, et al. The normal human optic nerve—axon count and axon diameter distribution. *Ophthalmology*. 1989;96:1325–1328.
42. Jonas JB, Muller Bergh JA, Schlotzer Schrehardt UM, et al. Histomorphometry of the human optic nerve. *Invest Ophthalmol Vis Sci*. 1990;31:736–744.
43. Ogden TE. Nerve fiber layer of the primate retina: thickness and glial content. *Vision Res*. 1983;23:581–587.
44. Mwanza JC, Kim HY, Budenz DL, et al. Residual and dynamic range of retinal nerve fiber layer thickness in glaucoma: comparison of three OCT platforms. *Invest Ophthalmol Vis Sci*. 2015;56:6344–6351.
45. Chen TC, Cense B, Miller JW, et al. Histologic correlation of in vivo optical coherence tomography images of the human retina. *Am J Ophthalmol*. 2006;141:1165–1168.
46. Tatham AJ, Weinreb RN, Zangwill LM, et al. The relationship between cup-to-disc ratio and estimated number of retinal ganglion cells. *Invest Ophthalmol Vis Sci*. 2013;54:3205–3214.
47. Hirasawa H, Tomidokoro A, Araie M, et al. Peripapillary retinal nerve fiber layer thickness determined by spectral domain optical coherence tomography in ophthalmologically normal eyes. *Arch Ophthalmol*. 2010;128:1420–1426.
48. Tun TA, Sun CH, Baskaran M, et al. Determinants of optical coherence tomography-derived minimum neuroretinal rim width in a normal Chinese population. *Invest Ophthalmol Vis Sci*. 2015;56:3337–3344.
49. Knight OJ, Girkin CA, Budenz DL, et al. Effect of race, age, and axial length on optic nerve head parameters and retinal nerve fiber layer thickness measured by Cirrus HD-OCT. *Arch Ophthalmol*. 2012;130:312–318.
50. Rhodes LA, Huisinck CE, Quinn AE, et al. Comparison of Bruch's membrane opening minimum rim width among those with normal ocular health by race. *Am J Ophthalmol*. 2017;174:113–118.
51. Seider MI, Lee RY, Wang D, et al. Optic disk size variability between African, Asian, white, Hispanic, and Filipino Americans using Heidelberg retinal tomography. *J Glaucoma*. 2009;18:595–600.
52. Bowd C, Zangwill LM, Weinreb RN, et al. Racial differences in rate of change of spectral-domain optical coherence tomography-measured minimum rim width and retinal nerve fiber layer thickness. *Am J Ophthalmol*. 2018;196:154–164.
53. Girkin CA, McGwin G, Long C, et al. Subjective and objective optic nerve assessment in African Americans and whites. *Invest Ophthalmol Vis Sci*. 2004;45:2272–2278.
54. Girkin CA, Liebman J, Fingeret M, et al. The effects of race, optic disc area, age, and disease severity on the diagnostic performance of spectral-domain optical coherence tomography. *Invest Ophthalmol Vis Sci*. 2011;52:6148–6153.